



Light quark jet quenching in higher-derivative gravity

Zi-qiang Zhang^{1,a}, Xiangrong Zhu^{2,b}, De-fu Hou^{3,c}

¹ School of Mathematics and Physics, China University of Geosciences (Wuhan), Wuhan 430074, China

² School of Science, Huzhou University, Huzhou 313000, China

³ Key Laboratory of Quark and Lepton Physics (MOE), Central China Normal University, Wuhan 430079, China

Received: 2 November 2022 / Accepted: 24 March 2023
© The Author(s) 2023

Abstract We study finite-coupling corrections on the energy loss of light quarks in strongly coupled $\mathcal{N} = 4$ super Yang–Mills (SYM) plasma. We perform the analysis by computing the stopping distance of an image jet induced by a massless source field, characterized by a massless particle falling along the null geodesic in Einstein gravity with curvature-squared (R^2) corrections. It turns out that the stopping distance in the R^2 theories can be larger or smaller than its SYM counterpart depending on the higher-derivative coefficients. Moreover, we evaluate the stopping distance in the Gauss–Bonnet background and find that increasing λ_{GB} (a dimensionless parameter in Gauss–Bonnet gravity) leads to a decrease in the stopping distance, thus enhancing the energy loss of light quarks, in agreement with previous findings for the drag force, jet quenching parameter, and the instantaneous energy loss of light quarks using shooting strings.

1 Introduction

Various findings from the quark gluon plasma (QGP) produced in heavy-ion collision experiments at the Relativistic Heavy Ion Collider (RHIC) and Large Hadron Collider (LHC) suggest that QGP is strongly coupled [1], and thus calculational tools beyond the perturbative quantum chromodynamics (QCD) are called for. Such tools are now available via the anti-de Sitter/conformal field theory (AdS/CFT) correspondence [2–5], which can relate the $\mathcal{N} = 4$ super Yang–Mills (SYM) theory in four dimensions to the type IIB superstring theory formulated on $\text{AdS}_5 \times S^5$ at the large 't Hooft coupling λ and large number of colors N_c limit. With this method, challenging questions about QCD in the strong coupling regime can be mapped to processes in theories of

gravity that are easily handled. Over the last two decades, the AdS/CFT correspondence has been used to study various aspects of QGP (see [6,7] for reviews with many phenomenological applications). One of its important applications is jet quenching: the rapid energy loss of highly energetic partons traversing QGP. For example, the energy loss of heavy quarks in SYM plasma has been studied by the drag force obtained from a trailing string moving in the dual geometry [8,9]. On the other hand, the energy loss of light quarks in SYM plasma has been discussed in different ways: for example, the jet quenching parameter extracted from a light-cone Wilson loop probing the infrared scale [10,11], the stopping distance of light quarks using falling string [12–16], and the instantaneous energy loss of light quarks using shooting strings [17,18].

It is known that string theory (or any quantum theory of gravity) may contain higher-derivative corrections because of stringy or quantum effects. Although we are not sure of the forms of higher-derivative corrections in string theory, we expect that generic corrections can occur due to the vastness of the string landscape [19]. For example, for the well-known $\mathcal{N} = 4$ SYM theory, the gravity dual corresponds to the type IIB string theory formulated on $\text{AdS}_5 \times S^5$. Using the relation $\sqrt{\lambda} = L^2/\alpha'$, the $\mathcal{O}(\alpha')$ expansion in type IIB string theory becomes the $1/\sqrt{\lambda}$ expansion in SYM theory, where L is the AdS radius and α' is the reciprocal of the string tension. The leading-order corrections, i.e., first higher-derivative corrections (commonly known as R^4 corrections), in $1/\lambda$ arise from stringy corrections to the type IIB tree-level effective action of the form $\alpha'^3 R^4$. On the other hand, the curvature-squared interactions (commonly known as R^2 corrections) to the gravity sector of AdS_5 are related to the leading $1/N_c$ corrections in the presence of a D7-brane [20–22]. Motivated by these vast string landscapes, various observables or quantities have been studied in higher-derivative gravity. For instance, the ratio of shear viscosity to entropy density [23–27], heavy

^a e-mail: zhangzq@cug.edu.cn (corresponding author)

^b e-mail: xrongzhu@zjhu.edu.cn

^c e-mail: houdf@mail.ccnu.edu.cn

quark potential [28–30], drag force [31–33], and jet quenching parameter [34,35] have been discussed under R^4 or R^2 corrections. Other interesting results can be found in [36–51]. To the best of our knowledge, although the calculation of the stopping distance under R^4 corrections was performed by [52], the R^2 corrections on this quantity have never been addressed in the literature. The intent of the present work is to fill that gap.

This paper is structured as follows. In the next section, we investigate the stopping distance of a light quark in general R^2 theories. In Sect. 3, we perform the analysis in Gauss–Bonnet (GB) gravity, a special kind of R^2 theory. The last part is devoted to conclusions and discussion.

2 Stopping distance with R^2 corrections

If considering the gravity sector in AdS_5 , the R^2 theories can be defined by the following action

$$I = \frac{1}{16\pi G_5} \int d^5x \sqrt{-g} \left[R + \frac{12}{L^2} + L^2(c_1 R^2 + c_2 R_{\mu\nu} R^{\mu\nu} + c_3 R_{\mu\nu\rho\sigma} R^{\mu\nu\rho\sigma}) \right], \quad (1)$$

where G_5 is the five-dimensional Newton constant, R is the Ricci scalar, $R_{\mu\nu}$ and $R_{\mu\nu\rho\sigma}$ are the Ricci tensor and Riemann tensor, respectively, and L is the AdS_5 radius at leading order in c_i , with $c_i \sim \frac{\alpha'}{L^2} \ll 1$. Other terms with factors of R or additional derivatives will be suppressed by higher powers of $\frac{\alpha'}{L^2}$ [25]. Note that c_i are arbitrary small coefficients, where c_3 is unambiguous at leading order while c_1 and c_2 can be arbitrarily varied by a metric redefinition [27].

A black hole solution for (1) can be written as

$$ds^2 = -f(r)dt^2 + \frac{r^2}{L^2}d\vec{x}^2 + \frac{1}{f(r)}dr^2, \quad (2)$$

where

$$f(r) = \frac{r^2}{L^2} \left(1 - \frac{r_0^4}{r^4} + \alpha + \beta \frac{r_0^8}{r^8} \right), \quad (3)$$

with

$$\alpha = \frac{2}{3}(10c_1 + 2c_2 + c_3), \quad \beta = 2c_3, \quad (4)$$

where r is the coordinate of the fifth dimension, and t, \vec{x} label the directions along the boundary at spatial infinity. In these coordinates, the boundary of the black brane geometry is $r = \infty$ and the horizon is located at $r = r_h$, which can be found by solving $f(r_h) = 0$. The parameter r_0 depends on α, β and r_h .

The temperature of the black hole is

$$T_{R^2} = \frac{r_0}{\pi L^2} \left(1 + \frac{1}{4}\alpha - \frac{5}{4}\beta \right). \quad (5)$$

Now we will study the jet quenching of a light probe by computing the stopping distance of a massless particle moving along the null geodesic in the background metric (2). Following [15,16] (see also [53–56]), the R-charged current can be generated by a massless gauge field in the corresponding gravity dual, and the induced current can then be considered as an energetic jet passing through the medium. Once the wave packet of the massless field falls into the horizon, the image jet on the boundary will dissipate and thus thermalize in the medium. Therefore, the stopping distance (or penetration depth) is defined as the distance for a jet passing through the medium before it thermalizes.

At the Wentzel–Kramers–Brillouin (WKB) approximation, one may consider the wave packet of the gauge field in the gravity dual localized in the momentum space. Then the wave function of the gauge field can be written as

$$A_j(t, z) = \exp \left[\frac{i}{\hbar} \left(q_k x_k + \int dz q_z \right) \right] \tilde{A}_j(t, z), \quad (6)$$

where q_k is the 4-momentum, which is conserved as the metric preserves the translational symmetry along the four-dimensional spacetime, z is the five-dimensional coordinate (note that the calculations of [15,16] were performed using the z coordinate, but one can go back to the r coordinate by the coordinate transformation $z = L^2/r$), q_z refers to the momentum along the bulk direction, $j, k = 0, 1, 2, 3$ are the four-dimensional spacetime coordinates, and $\tilde{A}_j(t, z)$ denotes the slowly varying with respect to t and z .

In the limit $\hbar \rightarrow 0$, the equation of motion of the wave packet will reduce to a null geodesic in the dual geometry,

$$0 = (ds^2) = dx^i g_{ij} dx^j + dz g_{zz} dz, \quad (7)$$

which results in

$$\frac{dz}{d\zeta} = \frac{1}{\sqrt{g_{zz}}} \left[-g_{ij} \frac{dx^i}{d\zeta} \frac{dx^j}{d\zeta} \right]^{1/2}, \quad (8)$$

where ζ denotes an affine parameter for the trajectory. The four-dimensional translation invariance

$$g_{ij} \frac{dx^j}{d\zeta} \quad (9)$$

is conserved and proportional to q_i , yielding

$$\frac{dx^i}{d\zeta} \propto g^{ij} q_j. \quad (10)$$

Then, dividing (10) by (8), one has

$$\frac{dx^i}{dz} = \sqrt{g_{zz}} \frac{g^{ij} q_j}{(-q_k g^{kl} q_l)^{1/2}}, \quad (11)$$

one can check that the null geodesic in (11) will remain unchanged even when one uses the Einstein frame.

To proceed, we compute the stopping distance. Assuming that the 3-momentum \vec{q} points in one of the \vec{x} directions, e.g., the x_3 direction, implying that $q_i = (-\omega, 0, 0, |\vec{q}|)$, where ω and \vec{q} are the energy and spacial momentum of the light quarks, respectively, plugging (2) into (11) and doing some algebraic transformations, the stopping distances of light quarks moving in SYM plasma with the effect of curvature-squared corrections is found as follows

$$x_{R^2} = \int_{r_h}^{\infty} \frac{dr}{r^2 \left(\frac{\omega^2}{|\vec{q}|^2} - \left(1 - \frac{r_0^4}{r^4} + \alpha + \beta \frac{r_0^8}{r^8} \right) \right)^{1/2}}, \quad (12)$$

where for convenience we have set the AdS radius L as unity. Note that if one takes $\alpha = \beta = 0$ in (12), the results of SYM [15, 16] will be recovered.

Now we analyze the R^2 corrections on the stopping distance. As was mentioned above, the exact interval of c_i has not been determined, which means that α and β are arbitrary constants (usually small). Ideally, one should discuss different values of α and β . In Figs. 1 and 2, we plot x_{R^2}/x_{SYM} versus α (or β) for various cases, where x_{SYM} denotes the corresponding stopping distance in SYM (i.e., without R^2 corrections). From these figures, one can see that increasing either α or β leads to an increase in x_{R^2}/x_{SYM} . Moreover, by comparing Figs. 1 and 2, one finds that α has a stronger effect than β . That is understandable, because α exists alone in $f(r)$ while β is multiplied by $(r_0/r)^8$, with $r_0/r < 1$. Moreover, with some chosen values of α and β , x_{R^2}/x_{SYM} can be larger or smaller than 1, indicating that R^2 corrections can increase or decrease the stopping distance depending on α and β , similar to the results of the drag force [32]. To summarize, given the uncertainty of α and β , exact or firm R^2 corrections on the stopping distance are hard to come by. However, the GB gravity, a special case of R^2 theories, may improve this situation. We will discuss this topic in the next section.

3 Stopping distance in Gauss–Bonnet gravity background

GB theory, the most general theory of gravity with quadratic powers of curvature in five dimensions, is defined by the classical action of the form [57]

$$I = \frac{1}{16\pi G_5} \int d^5x \sqrt{-g} \left[R + \frac{12}{L^2} + \frac{\lambda_{\text{GB}}}{2} L^2 \left(R^2 - 4R_{\mu\nu}R^{\mu\nu} + R_{\mu\nu\rho\sigma}R^{\mu\nu\rho\sigma} \right) \right], \quad (13)$$

where λ_{GB} is a dimensionless parameter, constrained in

$$-\frac{7}{36} < \lambda_{\text{GB}} \leq \frac{9}{100}, \quad (14)$$

where the upper bound originates from avoiding a causality violation in the boundary [26], while the lower bound comes from requiring the boundary energy density to be positive-definite [58].

A black hole solution for (13) is known analytically as [59]

$$ds^2 = -a^2 \frac{r^2}{L^2} f(r) dt^2 + \frac{r^2}{L^2} d\vec{x}^2 + \frac{L^2}{r^2} \frac{dr^2}{f(r)}, \quad (15)$$

with

$$f(r) = \frac{1}{2\lambda_{\text{GB}}} \left[1 - \sqrt{1 - 4\lambda_{\text{GB}} \left(1 - \frac{r_h^4}{r^4} \right)} \right], \quad (16)$$

and

$$a^2 = \frac{1}{2} (1 + \sqrt{1 - 4\lambda_{\text{GB}}}). \quad (17)$$

The temperature is given by

$$T_{\text{GB}} = \frac{ar_h}{\pi L^2}. \quad (18)$$

It is remarkable that the ratio of shear viscosity to entropy density in GB gravity [25–27]

$$\frac{\eta}{s} = \frac{1}{4\pi} (1 - 4\lambda_{\text{GB}}), \quad (19)$$

can violate the conjectured viscosity bound for $\lambda_{\text{GB}} > 0$.

The next analysis is parallel to the previous section, so we only show the final result. The stopping distance of light quarks in GB gravity is as follows

$$x_{\text{GB}} = \int_{r_h}^{\infty} \frac{dr}{r^2 \left(\frac{1}{a^2} \frac{\omega^2}{|\vec{q}|^2} - \frac{1}{2\lambda_{\text{GB}}} (1 - \sqrt{1 - 4\lambda_{\text{GB}}(1 - \frac{r_h^4}{r^4})}) \right)^{1/2}}. \quad (20)$$

In Fig. 3, we plot $x_{\text{GB}}/x_{\text{SYM}}$ as a function of λ_{GB} for the range $-\frac{7}{36} < \lambda_{\text{GB}} \leq \frac{9}{100}$ (note that the point of $\lambda_{\text{GB}} = 0$ is excluded from the numerical plot, since it appears in the denominator, but we will analyze it later using an analytical method). One can see that as λ_{GB} increases, $x_{\text{GB}}/x_{\text{SYM}}$ decreases. As we know, for light quarks, the greater the kinetic energy (or momentum), the larger the stopping distance. Therefore, one can conclude that increasing λ_{GB} leads to a decrease in the stopping distance, thus enhancing the energy loss of light quarks, consistent with the findings for the drag force [32], jet quenching parameter [33, 35], and the instantaneous energy loss of light quarks using shooting strings [18].

Moreover, from Fig. 3 one can see that positive (negative) λ_{GB} gives $x_{\text{GB}}/x_{\text{SYM}} < 1$ ($x_{\text{GB}}/x_{\text{SYM}} > 1$), indicating that the stopping distance in GB gravity will be smaller or larger than the SYM case depending on λ_{GB} . In particular, for $\lambda_{\text{GB}} = -7/36$, the ratio increases the SYM result by about

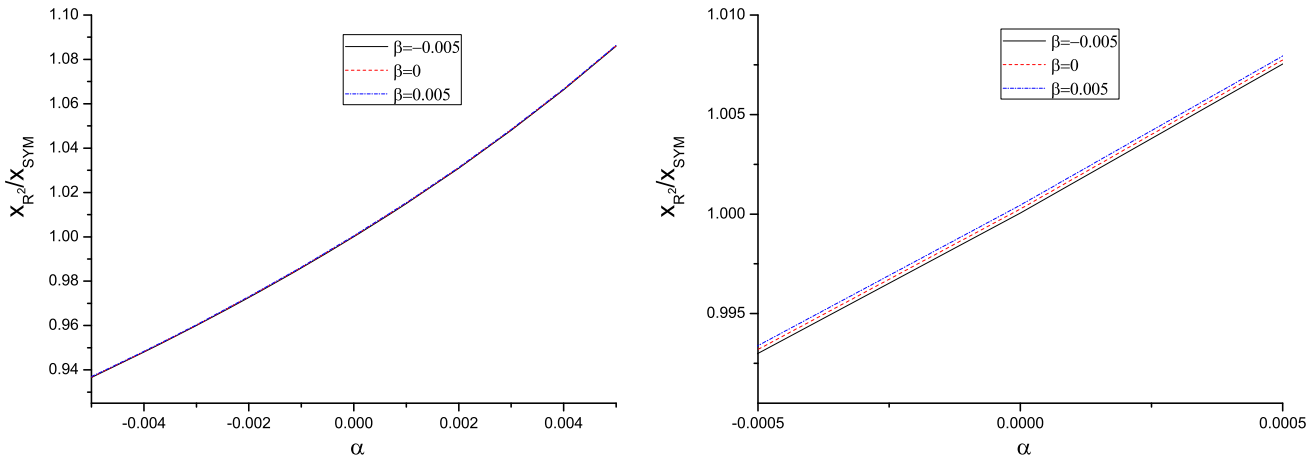


Fig. 1 x/x_{SYM} versus α with fixed β . Left: complete graph. Right: local image. Here we take $|\vec{q}| = 0.99\omega$

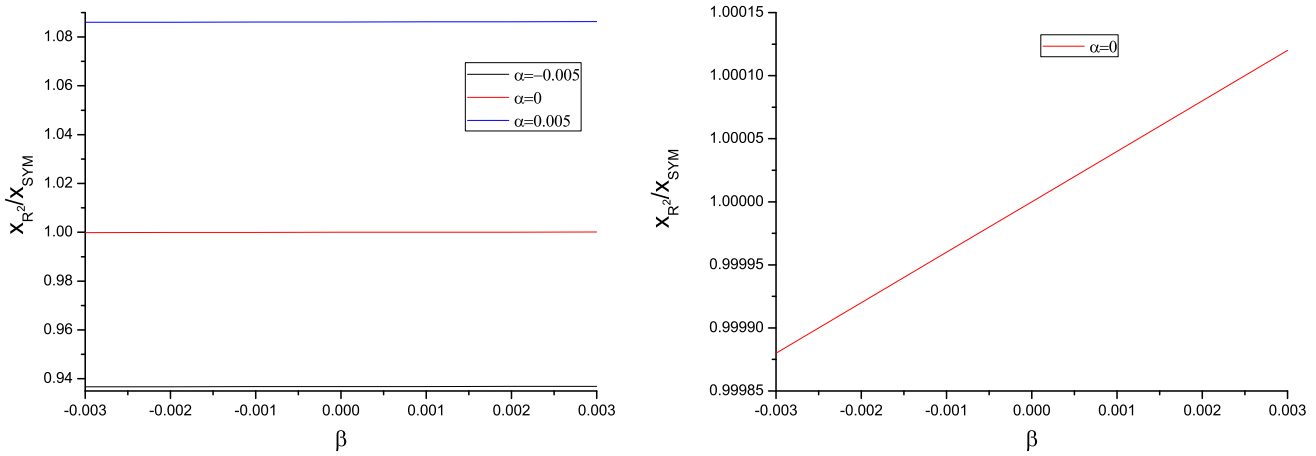


Fig. 2 x/x_{SYM} versus β with fixed α . Left: complete graph. Right: local image. Here we take $|\vec{q}| = 0.99\omega$

10 percent, while for $\lambda_{\text{GB}} = 9/100$ it decreases it by about 7 percent.

Now we discuss $\lambda_{\text{GB}} = 0$ for (20) using an analytical method. For $\lambda_{\text{GB}} > 0$, (20) can be rewritten as

$$x_{\text{GB}} = \int_0^1 dz \frac{L^2}{r_h} \frac{\sqrt{2\lambda_{\text{GB}}} |\vec{q}|}{(-q^2(1 - \sqrt{1 - 4\lambda_{\text{GB}}}) + \vec{q}^2(\sqrt{1 - 4\lambda_{\text{GB}}(1 - z^4)} - \sqrt{1 - 4\lambda_{\text{GB}}}))^{1/2}}, \quad (21)$$

where $z = r_h/r$ and $-q^2 = \omega^2 - \vec{q}^2$. Since $|\lambda_{\text{GB}}| < 1$, one can apply Taylor expansion (21) to the leading-order correction to $\lambda_{\text{GB}} = 0$ as

$$x_{\text{GB}} \simeq \int_0^1 dz \frac{L^2}{r_h} \frac{|\vec{q}|}{(-q^2 + \vec{q}^2 z^4 + \lambda_{\text{GB}}(-q^2 + 2\vec{q}^2 z^4 - \vec{q}^2 z^8))^{1/2}}. \quad (22)$$

Note that the above integrand is dominated by small z , with $z \sim (-q^2/\vec{q}^2)^{1/4}$. After dropping the z^8 term, (22) approximately [15, 16]

$$x_{\text{GB}} \simeq \int_0^\infty dz \frac{L^2}{r_h} \frac{|\vec{q}|}{(-q^2 + \vec{q}^2 z^4 + \lambda_{\text{GB}}(-q^2 + 2\vec{q}^2 z^4))^{1/2}} \propto (\omega^2/(-q^2))^{1/4} (1 + 3\lambda_{\text{GB}})^{-1/4}. \quad (23)$$

Similarly, for $\lambda_{\text{GB}} < 0$, one finds

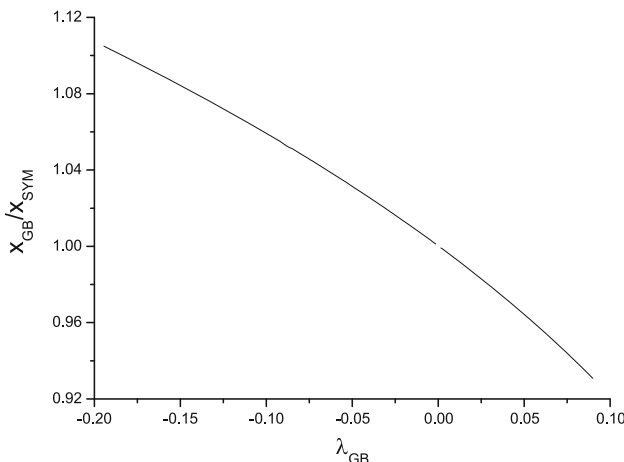


Fig. 3 x_{GB}/x_{SYM} versus λ_{GB} . Here we take $|\vec{q}| = 0.99\omega$

$$x_{GB} = \int_0^1 dz \frac{L^2}{r_h} \frac{\sqrt{-2\lambda_{GB}}|\vec{q}|}{(q^2(1 - \sqrt{1 - 4\lambda_{GB}}) + \vec{q}^2(-\sqrt{1 - 4\lambda_{GB}(1 - z^4)} + \sqrt{1 - 4\lambda_{GB}}))^{1/2}} \propto (\omega^2/(-q^2))^{1/4} (1 + 3\lambda_{GB})^{-1/4}. \quad (24)$$

(23) or (24) implies that for $\lambda_{GB} > 0$ ($\lambda_{GB} < 0$), the stopping distance of light quarks in GB gravity is smaller (larger) than its counterpart of SYM, consistent with previous numerical results.

4 Conclusion and discussion

We have studied the energy loss of light quarks in strongly coupled SYM plasma under R^2 corrections. We performed the analysis by computing the stopping distance of an image jet induced by a massless source field, characterized by a massless particle falling along the null geodesic in a general AdS₅ space with R^2 corrections and the GB background. For the general case, we found that the stopping distance with R^2 corrections can be larger or smaller than its SYM counterpart depending on α and β , and for smaller α and β , these corrections may not count for much. For the GB case, we observed that increasing λ_{GB} leads to a decrease in the stopping distance, thus enhancing the light quark energy loss, consistent with previous findings regarding the drag force [32], jet quenching parameter [33, 35], and the instantaneous energy loss using shooting strings [18]. Taking all this into account, one may draw a general conclusion that increasing λ_{GB} enhances the energy loss of heavy quarks and light quarks. However, it should be noted that the energy loss will be larger or smaller than its SYM counterpart because λ_{GB} can be positive or negative. Incidentally, the choice of $\lambda = 1$, including R^2 corrections with $\lambda_{GB} = -0.2$ (which gives

$\eta/s = 1.8/(4\pi)$), matches well with the nuclear suppression factor R_{AA} at LHC [18].

Also, the results may provide an estimate of how the energy loss changes with η/s at strong coupling. From (19) one can see that increasing λ_{GB} leads to a decrease in η/s , thus making the fluid more “perfect.” Here, we found that increasing λ_{GB} leads to increased energy loss. Thus, one may conclude that at strong coupling, as η/s decreases, the energy loss of both heavy quarks and light quarks is enhanced.

Acknowledgements This work is supported in part by the National Key Research and Development Program of China under contract no. 2022YFA1604900. This work also is supported by part by the National Natural Science Foundation of China (NSFC) under grant nos. 12275104 and 11890711. X.R. Zhu is supported by the Ministry of Science and Technology under grant no. 2020YFE0202001.

Data availability statement This manuscript has no associated data or the data will not be deposited. [Authors’ comment: This is a theoretical study and no experimental data has been listed.]

Open Access This article is licensed under a Creative Commons Attribution 4.0 International License, which permits use, sharing, adaptation, distribution and reproduction in any medium or format, as long as you give appropriate credit to the original author(s) and the source, provide a link to the Creative Commons licence, and indicate if changes were made. The images or other third party material in this article are included in the article’s Creative Commons licence, unless indicated otherwise in a credit line to the material. If material is not included in the article’s Creative Commons licence and your intended use is not permitted by statutory regulation or exceeds the permitted use, you will need to obtain permission directly from the copyright holder. To view a copy of this licence, visit <http://creativecommons.org/licenses/by/4.0/>.

Funded by SCOAP³. SCOAP³ supports the goals of the International Year of Basic Sciences for Sustainable Development.

References

1. E.V. Shuryak, Prog. Part. Nucl. Phys. **53**, 273 (2004)
2. J.M. Maldacena, Adv. Theor. Math. Phys. **2**, 231 (1998)
3. S.S. Gubser, I.R. Klebanov, A.M. Polyakov, Phys. Lett. B **428**, 105 (1998)
4. O. Aharony, S.S. Gubser, J. Maldacena, H. Ooguri, Y. Oz, Phys. Rep. **323**, 183 (2000)
5. E. Witten, Adv. Theor. Math. Phys. **2**, 253 (1998)
6. J.C. Solana, H. Liu, D. Mateos, K. Rajagopal, U.A. Wiedemann, [arXiv:1101.0618](https://arxiv.org/abs/1101.0618)
7. O. DeWolfe, S.S. Gubser, C. Rosen, D. Teaney, Prog. Part. Nucl. Phys. **75**, 86 (2014)
8. S.S. Gubser, Phys. Rev. D **74**, 126005 (2006)

9. C.P. Herzog, A. Karch, P. Kovtun, C. Kozcaz, L.G. Yaffe, JHEP **07**, 013 (2006)
10. H. Liu, K. Rajagopal, U.A. Wiedemann, Phys. Rev. Lett. **97**, 182301 (2006)
11. H. Liu, K. Rajagopal, U.A. Wiedemann, JHEP **03**, 066 (2007)
12. S.S. Gubser, D.R. Gulotta, S.S. Pufu, F.D. Rocha, JHEP **10**, 052 (2008)
13. P.M. Chesler, K. Jensen, A. Karch, Phys. Rev. D **79**, 025021 (2009)
14. P.M. Chesler, K. Jensen, A. Karch, L.G. Yaffe, Phys. Rev. D **79**, 125015 (2009)
15. P. Arnold, D. Vaman, JHEP **10**, 099 (2010)
16. P. Arnold, D. Vaman, JHEP **04**, 027 (2011)
17. A. Ficnar, S.S. Gubser, Phys. Rev. D **89**, 026002 (2014)
18. A. Ficnar, S.S. Gubser, M. Gyulassy, Phys. Lett. B **738**, 464 (2014)
19. M.R. Douglas, S. Kachru, Rev. Mod. Phys. **79**, 733 (2007)
20. O. Aharony, J. Pawelczyk, S. Theisen, S. Yankielowicz, Phys. Rev. D **60**, 066001 (1999)
21. O. Aharony, Y. Tachikawa, JHEP **01**, 037 (2008)
22. A. Buchel, R.C. Myers, A. Sinha, JHEP **03**, 084 (2009)
23. A. Buchel, J.T. Liu, A.O. Starinets, Nucl. Phys. B **707**, 56 (2005)
24. P. Benincasa, A. Buchel, JHEP **01**, 103 (2006)
25. M. Brigante, H. Liu, R.C. Myers, S. Shenker, S. Yaida, Phys. Rev. D **77**, 126006 (2008)
26. M. Brigante, H. Liu, R.C. Myers, S. Shenker, S. Yaida, Phys. Rev. Lett. **100**, 191601 (2008)
27. Y. Kats, P. Petrov, JHEP **01**, 044 (2009)
28. H. Dorn, H.J. Otto, JHEP **09**, 021 (1998)
29. J. Noronha, A. Dumitru, Phys. Rev. D **80**, 014007 (2009)
30. K.B. Fadafan, S.K. Tabatabaei, J. Phys. G **43**(9), 095001 (2016)
31. J.F. Vazquez-Poritz, [arXiv:0803.2890](https://arxiv.org/abs/0803.2890)
32. K.B. Fadafan, JHEP **12**, 051 (2008)
33. K.B. Fadafan, Eur. Phys. J. C **68**, 505 (2010)
34. J.D. Edelstein, C.A. Salgado, AIP Conf. Proc. **1031**(1), 207–220 (2008)
35. Z.Q. Zhang, D.F. Hou, Y. Wu, G. Chen, Adv. High Energy Phys. **2016**, 9503491 (2016)
36. S. Dutta, G.S. Punia, Phys. Rev. D **106**(2), 026003 (2022)
37. H. Krishna, D.R. Gomez, JHEP **11**, 139 (2021)
38. X. Wu, JHEP **12**, 140 (2019)
39. H.S. Reall, J.E. Santos, JHEP **04**, 021 (2019)
40. S. Waeber, JHEP **08**, 006 (2019)
41. S. Waeber, A. Schafer, JHEP **07**, 069 (2018)
42. S. Grozdanov, A.O. Starinets, P. Tadic, JHEP **06**, 180 (2021)
43. A. Buchel, Phys. Rev. D **98**(6), 061901 (2018)
44. J.C. Solana, S. Grozdanov, A.O. Starinets, Phys. Rev. Lett. **121**(19), 191603 (2018)
45. R. Nally, JHEP **09**, 094 (2019)
46. Z.Q. Zhang, Z.J. Luo, D.F. Hou, Ann. Phys. **391**, 47 (2018)
47. F. Li, G. Chen, Z.Q. Zhang, Chin. Phys. C **42**(12), 123109 (2018)
48. H. Ebrahim, S. Heshmatian, M.A. Akbari, Nucl. Phys. B **904**, 527 (2016)
49. S. Waeber, A. Schafer, A. Vuorinen, L.G. Yaffe, JHEP **11**, 087 (2015)
50. M.A. Akbari, Nucl. Phys. B **872**, 127 (2013)
51. S.I. Finazzo, J. Noronha, JHEP **11**, 042 (2013)
52. P. Arnold, P. Szepietowski, D. Vaman, JHEP **07**, 024 (2012)
53. B. Mller, D.-L. Yang, Phys. Rev. D **87**(4), 046004 (2013)
54. X.R. Zhu, Z.Q. Zhang, Eur. Phys. J. A **57**(3), 96 (2021)
55. Z.Q. Zhang, D.F. Hou, Eur. Phys. J. C **80**(10), 991 (2020)
56. Z.Q. Zhang, Phys. Lett. B **793**, 308 (2019)
57. B. Zwiebach, Phys. Lett. B **156**, 315 (1985)
58. D.M. Hofman, J. Maldacena, JHEP **05**, 012 (2008)
59. R.G. Cai, Phys. Rev. D **65**, 084014 (2002)